Defense Threat Reduction Agency
8725 John J. Kingman Road, MS
6201 Fort Belvoir, VA 22060-6201

DTRA-TR-13-55

TECHNICAL REPORT

Cascading Failures in Coupled Distributed Power Grids and Communication Networks

Approved for public release; distribution is unlimited

August 2013

HDTRA01-03-D-0009

Majeed M.Hayat, et al.

Prepared by:
Office of the Vice President for Research
University Strategic Partnership
MSC02 1660
1 University of New Mexico
Albuquerque, NM 87131

DESTRUCTION NOTICE:

Destroy this report when it is no longer needed.
Do not return to sender.

PLEASE NOTIFY THE DEFENSE THREAT REDUCTION AGENCY, ATTN: DTRIAC/ J9STT, 8725 JOHN J. KINGMAN ROAD, MS-6201, FT BELVOIR, VA 22060-6201, IF YOUR ADDRESS IS INCORRECT, IF YOU WISH THAT IT BE DELETED FROM THE DISTRIBUTION LIST, OR IF THE ADDRESSEE IS NO LONGER EMPLOYED BY YOUR ORGANIZATION.

REPORT DOCUMENTATION PAGE

Form Approved
OMB No. 0704-0188

1. REPORT DATE *(DD-MM-YYYY)*	**2. REPORT TYPE**	**3. DATES COVERED** *(From - To)*
00-08-2013	Technical	07/21/2010 - 04/30/2012

4. TITLE AND SUBTITLE

Cascading Failures in Coupled Distributed Power Grids and Communication Networks

5a. CONTRACT NUMBER
HDTRA1-03-D-0009

5b. GRANT NUMBER

5c. PROGRAM ELEMENT NUMBER

6. AUTHOR(S)

Majeed M. Hayat, Andrea Mammoli,Yasamin Mostofi and Patrick Bridges

5d. PROJECT NUMBER
1

5e. TASK NUMBER
26

5f. WORK UNIT NUMBER

7. PERFORMING ORGANIZATION NAME(S) AND ADDRESS(ES)

OVPR/University Strategic Partnership
MSC02 1660
1 University of New Mexico
Albuquerque, New Mexico 87131

8. PERFORMING ORGANIZATION REPORT NUMBER

OVPRED 798B

9. SPONSORING / MONITORING AGENCY NAME(S) AND ADDRESS(ES)

Defense Threat Reduction Agency
8725 John J. Kingman Road STOP 6201
Fort Belvoir,VA 22060
PM/James Reed

10. SPONSOR/MONITOR'S ACRONYM(S)

DTRA

11. SPONSOR/MONITOR'S REPORT NUMBER(S)

DTRA-TR-13-55

12. DISTRIBUTION / AVAILABILITY STATEMENT

Approved for public release; distribution is unlimited.

13. SUPPLEMENTARY NOTES

14. ABSTRACT

The University of New Mexico, through its University Strategic Partnership (USP) program, has supported the DTRA initiative aimed at advancing the state of the science and body of knowledge for "Network Adaptability from WMD Disruption and Cascading Failures." Using a combination of graph-theoretic dynamical modeling of cascading failures, optimal distributed control-algorithm design, and distributed estimation techniques, the team has studied how various communication network-based power measurement and control approaches impact the robustness and efficiency of power networks in the face of WMD-induced cascading failures.

15. SUBJECT TERMS

power grid networks WMD infrastructure

16. SECURITY CLASSIFICATION OF:			**17. LIMITATION OF ABSTRACT**	**18. NUMBER OF PAGES**	**19a. NAME OF RESPONSIBLE PERSON**
a. REPORT	**b. ABSTRACT**	**c. THIS PAGE**	UU	22	James Reed
Unclassified	Unclassified	Unclassified			**19b. TELEPHONE NUMBER** *(include area code)* 703-767-8793

CONVERSION TABLE

Conversion Factors for U.S. Customary to metric (SI) units of measurement.

MULTIPLY →	BY →	TO GET
TO GET ←	BY ←	DIVIDE
angstrom	1.000 000 x E -10	meters (m)
atmosphere (normal)	1.013 25 x E +2	kilo pascal (kPa)
bar	1.000 000 x E +2	kilo pascal (kPa)
barn	1.000 000 x E -28	meter^2 (m^2)
British thermal unit (thermochemical)	1.054 350 x E +3	joule (J)
calorie (thermochemical)	4.184 000	joule (J)
cal (thermochemical/cm^2)	4.184 000 x E -2	mega joule/m^2 (MJ/m^2)
curie	3.700 000 x E +1	*giga bacquerel (GBq)
degree (angle)	1.745 329 x E -2	radian (rad)
degree Fahrenheit	$t_k = (t^\circ f + 459.67)/1.8$	degree kelvin (K)
electron volt	1.602 19 x E -19	joule (J)
erg	1.000 000 x E -7	joule (J)
erg/second	1.000 000 x E -7	watt (W)
foot	3.048 000 x E -1	meter (m)
foot-pound-force	1.355 818	joule (J)
gallon (U.S. liquid)	3.785 412 x E -3	meter^3 (m^3)
inch	2.540 000 x E -2	meter (m)
jerk	1.000 000 x E +9	joule (J)
joule/kilogram (J/kg) radiation dose absorbed	1.000 000	Gray (Gy)
kilotons	4.183	terajoules
kip (1000 lbf)	4.448 222 x E +3	newton (N)
kip/$inch^2$ (ksi)	6.894 757 x E +3	kilo pascal (kPa)
ktap	1.000 000 x E +2	newton-second/m^2 ($N-s/m^2$)
micron	1.000 000 x E -6	meter (m)
mil	2.540 000 x E -5	meter (m)
mile (international)	1.609 344 x E +3	meter (m)
ounce	2.834 952 x E -2	kilogram (kg)
pound-force (lbs avoirdupois)	4.448 222	newton (N)
pound-force inch	1.129 848 x E -1	newton-meter (N-m)
pound-force/inch	1.751 268 x E +2	newton/meter (N/m)
pound-force/$foot^2$	4.788 026 x E -2	kilo pascal (kPa)
pound-force/$inch^2$ (psi)	6.894 757	kilo pascal (kPa)
pound-mass (lbm avoirdupois)	4.535 924 x E -1	kilogram (kg)
pound-mass-$foot^2$ (moment of inertia)	4.214 011 x E -2	kilogram-meter^2 ($kg-m^2$)
pound-mass/$foot^3$	1.601 846 x E +1	kilogram-meter^3 (kg/m^3)
rad (radiation dose absorbed)	1.000 000 x E -2	**Gray (Gy)
roentgen	2.579 760 x E -4	coulomb/kilogram (C/kg)
shake	1.000 000 x E -8	second (s)
slug	1.459 390 x E +1	kilogram (kg)
torr (mm Hg, 0^0 C)	1.333 22 x E -1	kilo pascal (kPa)

*The bacquerel (Bq) is the SI unit of radioactivity; 1 Bq = 1 event/s.

**The Gray (GY) is the SI unit of absorbed radiation.

Final Report

Contract: DTRA01-03-D-0009-0026
Project title: Cascading Failures in Coupled Distributed Power Grids and Communication Networks
PI: Majeed M. Hayat; Co-PIs: Andrea Mammoli, Yasamin Mostofi and Patrick Bridges
University of New Mexico
Date of Report: May 5, 2012

0. Abstract

Emerging distributed power-grid systems will integrate tightly-coupled networks, namely a power grid and a communication network, to provide distributed power monitoring and control. While distributing power monitoring and control away from a central site enhances the robustness of the power-grid to multiple, dispersed failures and attacks, such communication-based distributed control schemes can introduce complex cascading failure scenarios in the face of large-scale WMD attacks. The objective of this project is to model and analyze the interactions between coupled communication networks and power distribution grids so that potential cascading failures in the composite complex bi-infrastructure network can be examined, analyzed and avoided. This fundamental research work is motivated by fundamental challenges presented by potential distributed power-grid topologies and structures currently under discussion in the power community. This leads to a framework for understanding the subtle interactions between coupled power-grid and communication networks and their effects on cascading failures. Using a combination of graph-theoretic dynamical modeling of cascading failures, optimal distributed control- algorithm design, and distributed estimation techniques, we will study how various communication network-based power measurement and control approaches impact the robustness and efficiency of power networks in the face of WMD-induced cascading failures. The project uses this abstraction to characterize cascading failures in terms of system parameters such as power-line/substation capacity, communication connectivity and delay, and network/grid topology, as well as parameters related to distributed energy resources such as generation, storage, and demand response. The proposed technical approach will then provide us with a novel design framework for increasing adaptability and robustness of smart power grids to WMD-induced cascading failures. It is to be noted that funding for this project was offered only for the first year of the original three-year project.

1. Objectives

The objective of the proposed work is to develop a mathematical theory to analyze cascading failures in coupled distributed power grids and communication networks resulting from WMD-induced time/space correlated damage to the power and communication infrastructure. The predictive capability of the mathematical framework will be used (1) to establish an understanding of the vulnerabilities associated with cascading-failure effects in distributed approaches for power delivery, and (2) to optimize the control-agent and power redistribution design as well as power grid and communication network topology to minimize cascading failures.

2. Specific Tasks according to the Statement of Work

This effort consisted of five tasks as listed below.

Task 1. Graph-theoretic modeling of cascading failures in distributed power grids in face of time/space correlated WMD-induced damage.
Task 2. Build simulation capabilities by porting GridLAB-D to high-performance computational platforms and coupling it with the OmNet++ network simulator.
Task 3. Understand the logical coupling of the communication network and the power grid.
Task 4. Formulate graph-optimization problem for the communication-network topology for robust communication under WMD-induced failures.
Task 5. Perform simulation-based analysis of smart power grids for system-parameter identification and optimization.

3. Status of effort

All tasks have been completed. The project resulted in three IEEE conference papers on power systems. These papers are attached to this report in the Appendix.

4. Accomplishments/New Findings

Here we present the scientific and technical accomplishments categorized according to the tasks listed above.

4.1. Graph-theoretic modeling of cascading failures in distributed power grids in face of time/space correlated WMD-induced damage.

4.1.1 Graph-theoretic abstraction of power grids

As a starting point, we identified key power grid components, parameters and their dynamics. We abstracted the power grid as a graph consisting of nodes (generators and substations) and transmission lines connecting the nodes. We considered the power flow distribution in this graph based on the physics electricity law. However, the complexity of keeping track of the detailed power grid state and its power flow dynamics in an analytical model is $O(2^n)$, where n is the number of transmission lines in the power system. This rendered our initial abstraction non-scalable to large grids. To alleviate this problem, we used the novel idea of equivalence classes in order to reduce the complexity. To do so, we first identified, through simulations, certain power grid parameters which play a critical role in the dynamics of load redistribution and cascading failures. (We had built our simulation capabilities

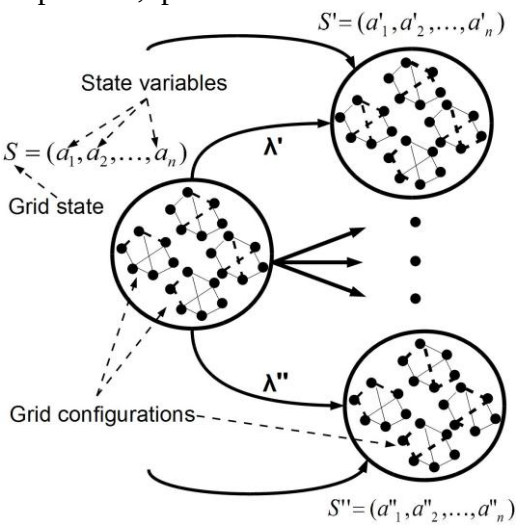

Fig. 1. Grid configuration, grid state and the transition between the grid states.

using MATPower [4], a package of MATLAB m-files as well as GridLab-D for the distribution level. More details on the simulators are given later in this report, see Section 4.2.) Based on our simulation results, we discovered that the number of failed transmission lines, maximum capacity of the failed lines and the grid-loading ratio (which is defined as the ratio of the total demand over the total generation capacity of the grid) affect, to a large degree, cascading failures in power grids. The use of number of failed lines and the maximum capacity of the failed lines as a descriptor of the "state" of the grid enabled us to partition the collection of all power grid configurations into a collection of equivalence classes. Therefore, this partitioning of the entire collection of grid configurations, as depicted in Fig. 1, reduced the complexity of tracking the dynamics of the power grid to $O(n)$. In Fig. 1, each large circle represents a grid state and the topological graphs with working and failed lines inside the circles representing different grid configurations with the same number of failures and the same maximum capacity of the failed lines.

4.1.2 A Probabilistic model for the dynamics of cascading failures and blackouts in power grids

With the simplified abstraction of the power grid at hand, we developed a novel probabilistic approach based on stochastic-regeneration theory to model the dynamics of cascading failures in power grids. The model characterizes the probability of reaching a blackout of an arbitrary size in any time interval starting from an initial grid state with random initial failures. By using this model, we can derive the distribution of the blackout size in power grids. This model utilizes the power flow distribution dynamics, graph-theoretic abstraction and our defined equivalence classes based on the key power grid parameters affecting the cascading failures. In the following we present some of the equations and the theorem we developed for this model.

We use the notation $B_{(C\max,F)}(t, M)$ to represent the probability of reaching blackout size M or larger (a blackout with M or more line failures) in a time interval t and initial grid state $S = (C_{\max}, F)$ and initial grid-loading ratio, $R_{D/G}$. Here, $C_{\max}$ and F are the maximum capacity of the failed lines and the number of the failed lines in the grid, respectively.

Note that when $F \geq M$ then $B_{(C\max,F)}(t, M) = 1$. Now, we consider the case $F < M$ and derive integral equations describing the probability. By exploiting the properties of conditional expectations and renewals, we can write

$$B^{R_{D/G}}_{(C_{\max},F)}(t,M) = (1 - P_{stab}(S, R_{D/G})) \times \int_0^t B^{R_{D/G}}_{(C_{\max},F)}(t, M \mid \tau = s)\, f_\tau(s) ds\,,$$

where $f_\tau(s)$ is the probability density function (pdf) of τ which is the time of the *first* event occurring following an initial condition at (e.g., the *first* line failure). Note that $B_{(C\max,F)}(t, M \mid \tau = s)$ is the conditional probability of reaching a blackout with at least M failures in the time interval t given that τ is equal to s (recall that the first event occurs at s). We write this probability as

$$B^{R_{D/G}}_{(C_{\max},F)}(t, M \mid \tau = s) = P\{\tau = W \mid \tau = s\} B^{R_{D/G}}_{(C_{\max},F)}(t, M \mid \tau = s, \tau = W) +$$
$$\sum_{i \in L} P\{\tau = U_i \mid \tau = s\} B^{R_{D/G}}_{(C_{\max},F)}(t, M \mid \tau = s, \tau = U),$$

where U_i and W are different events corresponding to the failure of a line with larger capacity than $C_{\max}$ and failure of a line with the same capacity as $C_{\max}$, respectively. Now, we state the following theorem on the probability of a blackout of size M.

Theorem-The probability of reaching a blackout of size M or larger in a time interval t and from an initial state $S = (C_{\max}, F)$, where $F < \mathrm{M}$, and initial grid-loading ratio, $R_{D/G}$, is characterized by the following differential equation:

$$\frac{dB^{R_{D/G}}_{(C_{\max},F)}(t,M)}{dt} = -\lambda(S,R_{D/G})B^{R_{D/G}}_{(C_{\max},F)}(t,M) +$$
$$(1-P_{stab}(S,R_{D/G}))(\lambda_w(S,R_{D/G})B^{R_{D/G}}_{(C_{\max},F+1)}(t,M)) + \sum_{i\in L}\lambda_{U_i}B^{R_{D/G}}_{(C_{\max},F)}(t,M)).$$

A key feature of this model is that the transition rates between the states of the model (which represents the rate of dynamics of the cascading failures) depend on the state of the system. This model is among the very few models which represent the evolution of the cascading failure probability in time. This means the results of the analytical model shows how fast the probability of cascading failure increases from an initial state in the absence of efficient corrective actions. The parameters of this model are estimated based on the Monte Carlo power-system simulations. The transition probability and the stability probability of the power system states are presented as functions of capacity of the failed lines and the number of failed lines in Fig. 2 and Fig. 3, respectively. Furthermore, this model enabled us to consider the effect of multiple correlated failures (WMD-induced damage) through the states with multiple failures as the initial state of the power system.

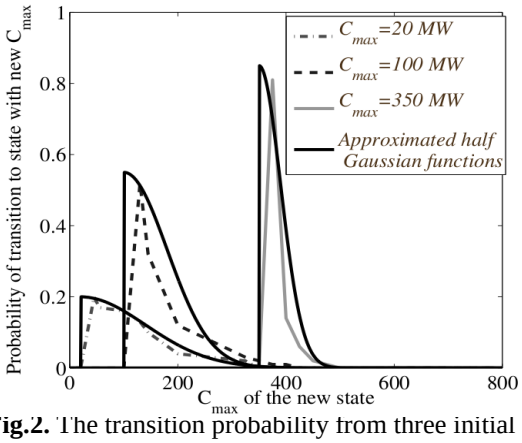

Fig.2. The transition probability from three initial states with different maximum capacity of the failed lines to different possible states S′ with $C'_{\max} > C_{\max}$.

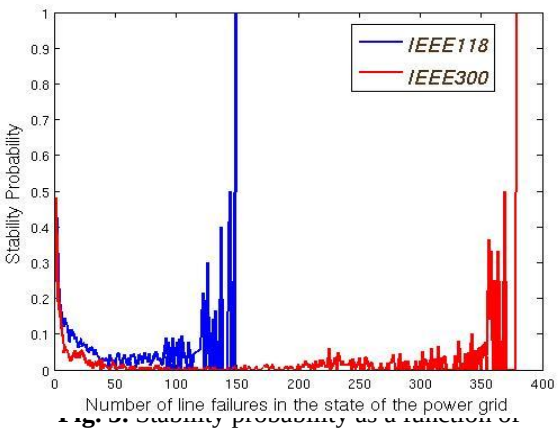

Fig. 3. Stability probability as a function of number of failures in the state.

Our paper on this model which was submitted to the IEEE PES General Meeting 2012 has been accepted [1].

4.1.3 Verification of the analytical results with power grid simulations

We used our power-system simulation capabilities to simulate the cascading failure behavior in power grids such as IEEE 118 and IEEE 300 test cases. The observed

behavior by the simulation of these two systems was similar. As an example, the effects of the capacity of the initial transmission line failures and the number of line failures on stability of the power grid were similar in these two test cases. We further applied the regeneration-theory model to power grid IEEE 118. The results of the analytical model are in agreement with Monte Carlo simulations performed with the IEEE 118-bus system (please see Fig. 4 for a representative result). Thus, we can conclude that the model is successful in capturing and predicting the power-grid cascading failure. In particular, the analytical model enabled us to predict the blackout probability for different initial failure(s) and with different system parameters. A representative set of graphs showing the capability of the model to predict cascading behavior is shown in Fig. 5 below.

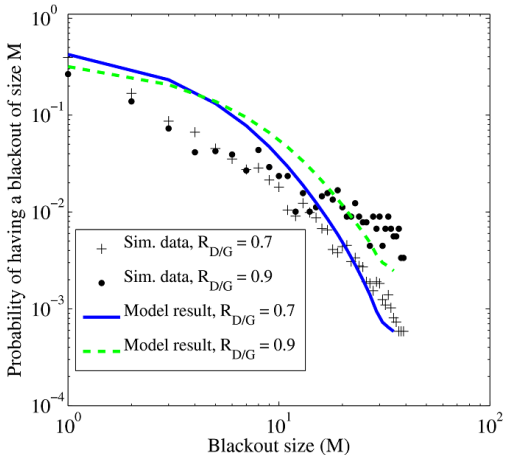

Fig. 4. Prob. of having a blackout of size *M*, as a function of *M*, for IEEE 118-bus system. Solid and dashed lines represent calculated results for our model and dots and crosses represent Monte Carlo simulation values.

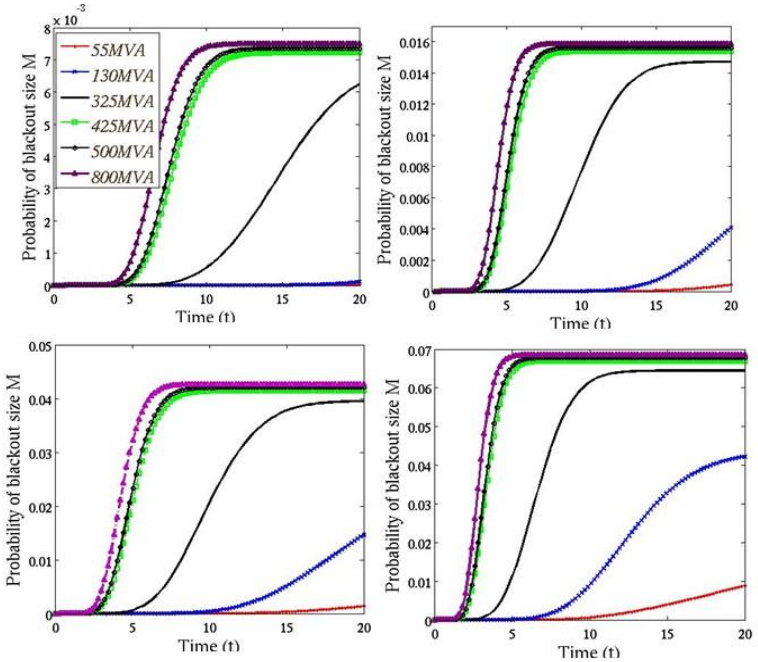

Fig. 5. Calculated values of the probability of reaching blackouts with M = 40 or more in IEEE 118-bus system in 20 min. interval. Each curve is parameterized by the max. capacity of failed lines. (a) Initial state has 5 failures and $R_{D/G}$ = 50%, (b) initial state has 10 failures and $R_{D/G}$ = 50%, (c) initial state has 5 failures and $R_{D/G}$ = 90%, and (d) initial state has 10 initial failures and $R_{D/G}$ = 90%.

The results in Fig. 5 show quantitatively that in cases where the maximum capacity of the failed lines is large (> 400MW), the probabilities of the blackouts are larger than those corresponding to other cases where the maximum capacity is low. The same effect can be seen when the number of initial failures is large. As expected, in cases where the grid-loading ratio is large the probabilities of blackouts are also large compared to those with smaller values of the grid-loading ratio. Moreover, the probability increases much faster in time than other initial grid states. These plots represent evolution of the risk of blackout in time and how quickly the risk increases with time if no action is taken as time passes. The results are consistent with the physical concepts used in the model and also simulation results.

4.2. Building simulation capabilities by porting GridLAB-D to high-performance computational platforms and coupling it with a network simulator

4.2.1 Transmission level simulations

We used MATPower, a package of MATLAB m-files, to simulate the power system transmission layer. The transmission layer is of particular interest to this project as cascading failures are attributes of this layer. MATPower helped us solve optimal power-flow problems and simulate the power flow distribution over the grid. We performed several simulations on IEEE 118 and IEEE 300 test cases with MATPower in order to see the effect of various parameters affecting cascading failure, specifically those pertaining to overload conditions. As a real power system example, we decided to use the ERCOT (Texas) power transmission network because it is large enough to exhibit cascading

effects and it is largely self-contained (with only a few connections to external network), yet it is treatable for our studies. We extracted relevant data from the ERCOT transmission network: from GIS to a format that is compatible with MATPower. However, there was insufficient information in the data available to us on the Texas grid. To remedy this deficiency, we used our understanding of the topology, load substations, and generators, to generate good-faith estimates of the missing information, which enabled us to successfully simulate the power flow over our augmented version of the Texas power grid. We also simulated some scenarios of cascading failure over the Texas power grid.

4.2.2 Distribution level simulations

The GridLAB-D source code was compiled on the high-performance machine Pequena (available to this project through collaboration with Dr. Susan Atalas, Director of UNM's Center for Advanced Research Computing, CARC), an SGI-Ultrix platform with 2 TFLOPS of peak processing power. We worked with developers at PNNL (regional power company) to resolve several issues related to running Gridlab-D under Linux in general or 64-bit Linux. We built models of real-life distribution grids from data provided to us by our local utility company, PNM. We also built models for two distribution grids, each with approximately 2000 loads. We completed the model of a real distribution feeder in Albuquerque, NM, which will allow us to determine realistic load-shedding scenarios that can be achieved using smart grid controls.

We considered loads that can be controlled by adjusting the power consumption at the "end user" level (residential and commercial) via "smart grid" controls. We investigated by means of GridLAB-D how much control can be exerted at the end user level under various scenarios, ranging from the status quo to a futuristic distribution grid with "smart" load, including PHEV, appliances that can respond to price signals, and "community" storage in the form of large batteries. Our models enabled us to indicate how much load reduction can be achieved at substation nodes, how long the load reduction can last, and how fast it can happen. We used the results from the distribution grid simulations to determine the overall time and magnitude response characteristics of a substation (a class of nodes in our transmission networks) to a load shed request. We also used MATPower to implement certain load-shedding operations. Load shedding is implemented by the optimization on the generation and load distribution over the power grid. Another significant accomplishment is that we were able to model the TRAMWAY11 distribution feeder in both GridLAB-D and OpenDSS, performing a complete simulation of daily operation, including a number of distributed (residential) PV generators. This enabled us to simulate realistic load shedding events, as described by statistical distributions of load shedding capacity of distributed resources, which collectively provide a response to a load shedding request at the transmission level. Our load control model and the results on their effects on the power grid are published in [2].

4.2.3 Simulating coupling between communication network and power system simulations

We studied various parameters related to the communication network that may affect the cascading failures in its coupled power grid. Example of such parameters are the average network latency, bandwidth limitations, and queuing of messages during high levels of

congestion. We included communications module components in our GridLab-D model and test their capacity to perform load-shedding operations. We also performed parameter tests to investigate the effect of latency due to faults in the network as a consequence of attacks. We specified a simple set of data that needs to be exchanged between the communication network simulator and MATPower/GridLab-D to provide the necessary communication latency and connectivity information to evaluate various control strategies. In our studies we adopted the realistic assumption designed control signals are transferred over the communication network upon a communication request. At that point, communication network simulator simulates the outcome of the communication request. This reset operating conditions (via the input file) for MATPower/GridLAB-D, until the next communication request, and so on. We also improved our understanding of the IEEE test grids by including topological information about these grids in our communication network simulations, which previously only included node connectivity and physical distance between nodes. This allowed us to analyze the geographical distributions of generators and loads, allowing us to locate control hubs in a practically reasonable way.

4.3. Understand the logical coupling of the communication network and the power grid

4.3.1 Control and communication system structure design

We considered the control and communication system of the power grid as a hierarchical system. Control and communication systems of the transmission network and the distribution network of the power grid are two levels of this hierarchy. Since large blackouts and cascading failures are attributes of the transmission network in power grids, we studied the cascading behaviors in this level as an important step in understanding cascading phenomenon. We assumed that the control over the distribution network, placed below the substations of the transmission network, would perform the local control actions as well as implementing necessary remote control signals. We decomposed the transmission grid into sub-systems based on the control regions defined over it. We assumed that in each sub-system, the control regions utilized controlling and monitoring agents. These agents were located on top of the communication nodes and operate and communicate over the communication system spanned over the control region. Examples of controlling agents are control relays and remote terminal units (RTUs), which performed local control/automation and execute remote control signals from system control center (SCC). The SCC is the critical control center, which makes region-wide decisions and may have backup centers to solve the single point of failure problem. However, at each time only one SCC is the responsible control center for the region. Where to locate the SCC in the control/communication system of a power grid is an important decision in designing reliable control/communication systems. Hence, we utilized the clustering algorithms to identify the best places (according to required power grid and communication characteristics we defined) to locate the SCC and its backup

systems over the power grid. Examples of the metrics we used in the clustering algorithm are power volume passing through different points of the grid and the reachability, connectivity and geographical proximity to the grid components. To reiterate, the communication network includes two categories of heterogonous nodes. The first category contains *monitoring nodes* that collect and relay grid-information. The second category contains only a few *decision/control nodes* that are directly associated with the high-level control centers described above

Note that there may not be necessarily a direct (one-to-one) correspondence between the nodes in the communication network and the power grid components. For example, a communication node may be associated to a subset of power-grid components or there may be auxiliary nodes covering a subset of components. This gave us flexibility in the design of a robust communication network to improve reliability and robustness. We tried communication networks with different characteristics such as degree of connectivity.

4.3.2 Logical coupling of communication network and the power grid

We studied the cascading phenomenon in the power grids under the scenarios, which the initial disturbances in the power grid are accompanied by other system vulnerabilities such as failures of the communication and control systems that transmit and implement critical control signals. In this study, the vulnerabilities in the control and communication system were coupled with the load shedding mechanism and their effects on power-grid cascading behavior were revealed by means of simulation. Load shedding is a critical control action when the system must be reconfigured to accommodate the disturbances on the power grid. We modeled the vulnerabilities in the control/communication systems (communication system failures, control system failures, and physical and policy-based limitations) by formulating an optimization problem for the load-shedding control with new constraints to capture these vulnerabilities. This approach relies on the direct modeling of control/communication system vulnerabilities within the load-shedding formulation. It is a simple yet effective approach for coupling the power grid with the control/communication systems without dealing with the complexities associated with integrating communication system and power-grid simulators. We studied various scenarios of failures in the control and communication network and their effect on the cascading failures in the power grid. We also considered various scenarios with different topological location of the failures in the communication network. The results of these studies have been accepted to publish in IEEE PES General Meeting 2012, [3]. The results on the effect of losing load shedding control on the cascading failure are presented in Fig.6. According to the results presented in Fig. 6, for a fixed amount of uncontrollable loads over the grid, the scenario for which we totally lose control over certain load buses results in a more severe cascading effect compared to that for the scenario where we lose control over a portion of the loads in the load buses. Furthermore, in the presence of control/communication vulnerabilities, lines have increased chance of becoming overloaded and hence fail, which causes the load buses to be disconnected from the grid.

Therefore, the total amount of unserved loads in these cases are larger than that in the case when controlled load reduction (necessary load shedding) is performed.

Figure 7 represents the effects of different topological distribution of uncontrollable loads over the power grid. In Fig.7 we consider scenarios with five load buses with uncontrollable loads randomly selected over the grid. In each sub figure of Fig. 7 we have shows the results on the number of failures due to cascading phenomenon for each of the 10,000 realizations of the randomly selected load buses with uncontrollable loads. Note that each point in each of the plots corresponds to one realization (from all the combinations of 5 buses chosen from all the load buses in the grid) of the five randomly selected load buses with uncontrollable loads. The results in Fig.7 show that both the topological location of the transmission line failures and the topological location of the failures in the control/communication system affect the cascading behavior of the power grid. In Fig.7 we have also looked at the effects of spatial inhibition and clustering among the uncontrollable load buses. These effects can be important due to the nature of certain disaster events that may affect the power grid and their control/communication systems. (In Fig.7, the square markers correspond to scenarios with inhibition and circles correspond to the scenarios with clustering.) We observe that when there is clustering effect in the distribution of the uncontrollable load buses the occurrence of cascading failures are less likely compared to the case in which there is inhibition effect. This may be attributed to the ability of the power grid to isolate the problem locally in the case when the uncontrollable buses are within close proximity of one another, which may impede the propagation of subsequent failures through the grid.

Probability of cascading failure as a function of the minimum total capacity of the connected lines for three different number of load buses with uncontrollable loads over the grid is shown in Fig. 8. When the minimum total capacity of the lines connected to load buses with uncontrollable loads is above a threshold then the probability of having cascading failures drops sharply. This phenomenon is shown in Fig. 8, where we show the probability of having ten or more failures beyond the initial three failures for three values for the number of load buses with uncontrollable loads. This can be explained as follows. Since it is assumed that the loads on the buses with uncontrollable loads are fixed if they have lines with lower capacities, there is a higher probability of overloading such line in the case of contingencies. Moreover, it can also be seen from Fig. 8 that the probability of having cascading failures increases with the number of uncontrollable load buses.

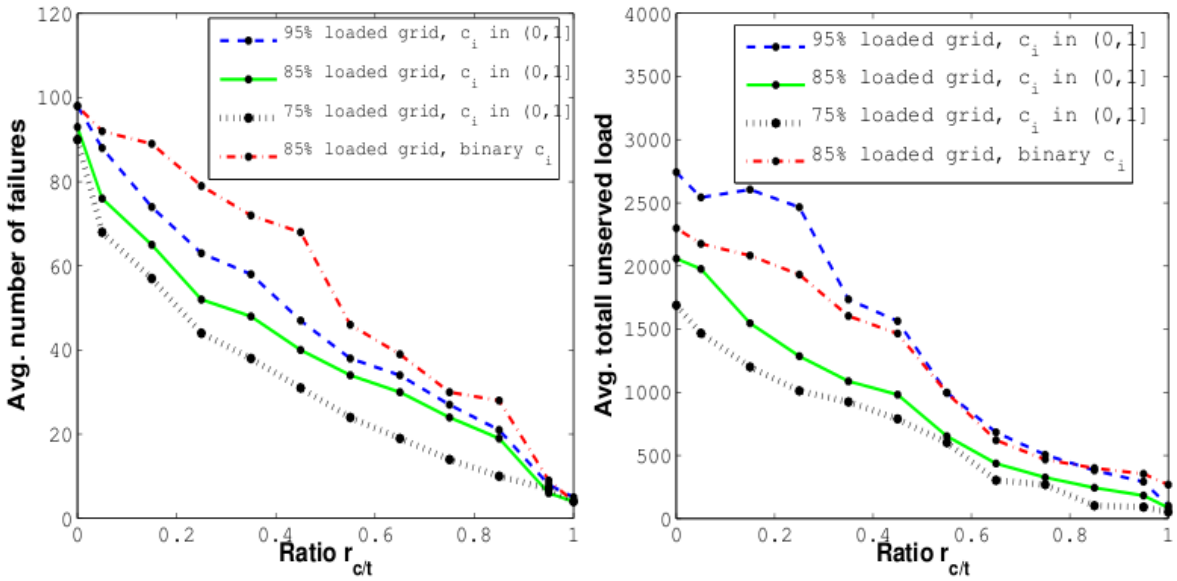

Fig. 6. Average (a) number of failed lines, and (b)total unserved load, due to cascading failures as a function of the ratio of total controllable loads over the total load in the grid.

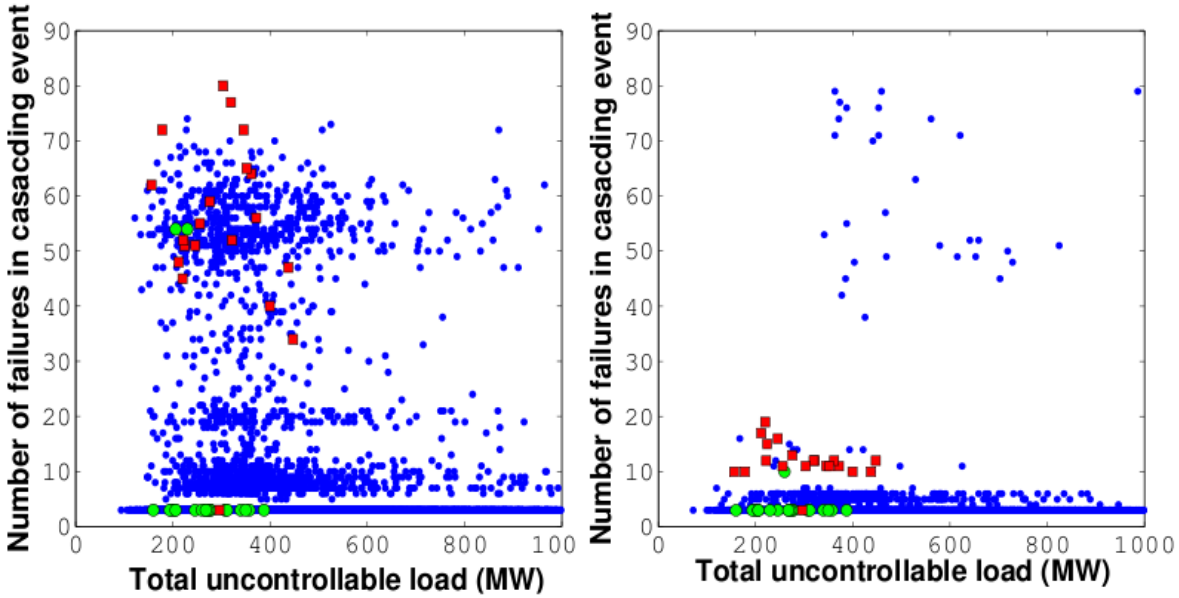

Fig.7. Cascading behavior of the grid for distributions of load buses with uncontrollable loads over the grid for two scenarios of initial failures

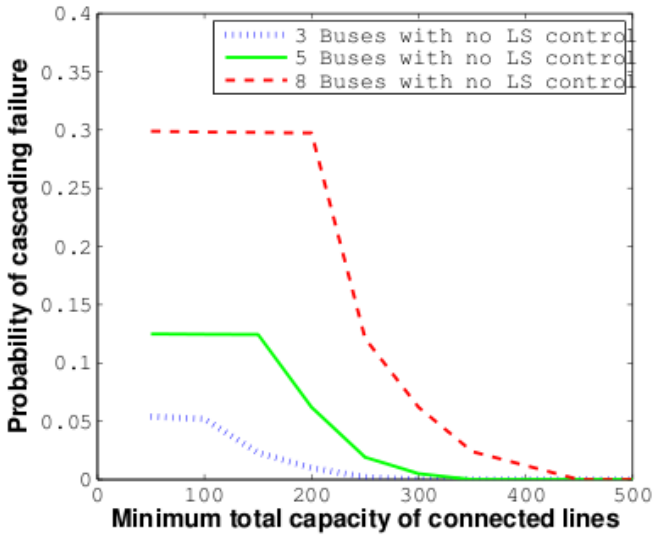

Fig. 8. Probability of cascading failure as a function of the minimum total capacity of the connected lines for three different number of load buses with uncontrollable loads over the grid.

4.4. Formulation of graph-optimization problem for the communication-network topology for robust communication under WMD-induced failures

The topology of the communication network, comprising all the nodes and the connecting communication lines, designed to maximize reachability between the decision/control nodes and the monitoring nodes especially in the case of component failure in the communication network. The design of the communication network structure and topology includes discovering the number of required nodes and links and their topological placement, as well as resilient communication protocols. We designed optimized communication networks overlaying the IEEE-118 power grid. Using the network connectivity as a metric as well as the clustering algorithm developed in the previous task, optimization was performed to identify the best five locations (nodes) for locating the SCCs described above. This enabled us to create scenarios for robust communication, with the most robust location used as the main SCC and lower-rank, backup SCCs used thereafter in the event of disruption in the communication due to a WMD attack. Random and correlated node-failure patterns were induced in the network simulations as the optimization was performed. In the communication network design we used a number of topologies, including random topologies, full mesh and scale-free topologies with various average nodes degrees (number of edges at a node). We observed that power grids with coupled communication systems, which have higher connectivity probability in the case of failures, are more robust in the case of contingencies. In addition, we observed that the topological location and characteristics of the failures affect the cascading behaviors in the power grid. The reachability information extracted from these studies can be fed into the power-grid analytical model and the power

simulators. The optimal approach for such data collection graphs is a Steiner tree, and the construction of optimal Steiner trees is known to be computationally intractable. As a result, both offline and online mechanisms for constructing robust communication topologies that approximate optimal graphs are needed. We worked on optimizing data aggregation and transport in unreliable networks by determining appropriate gradient-based routing functions to optimize data delivery reliability and efficiency, and comparing the resulting routing structures at small scales with offline-computed optimal routing trees. We studied the effect of structured and unstructured communication networks on the robustness of smart grids in the face of WMD attacks.

4.5 Perform simulation-based analysis of smart power grids for system-parameter identification and optimization

With increasing penetration of renewable power generation, primarily from centralized wind farms (transmission level) or from PV (primarily at the distribution level), there is a need to increase the capacity of demand response (DR) programs to absorb intermittency from these resources. The implementation of these programs, with associated control strategies, *is synergistic with the requirements of securing the transmission grid from WMD attacks*.

Our investigation of cascading failure mechanisms has shown that load shedding can be an effective method of reducing the likelihood of cascading failure, if implemented in a timely manner. However, currently load shedding are generally implemented by an operator manually, following a request from a system operator. Moreover, requests are subject to human judgment, and sometimes fail to be implemented correctly, in a timely manner and/or in their entirety. An automated response, making use of energy storage, would have two benefits: first, its implementation would not depend on human judgement. Second, its impact on end users would be less severe. For example, storage units (thermal storage, community electric storage, utility-scale electric storage) may be deployed to produce a certain level of load shed, rather than resorting to rolling black-outs or brown-outs.

There are a number of challenges in the implementation of automated, fast acting load shedding strategies for WMD protection. First, the mechanism must be compatible with "normal" grid operation mechanisms. Second, the mechanism must be compatible with local regulations. For example, control by real-time pricing (RTP) may be possible in some regions, but not others. Where RTP is not available, other control mechanisms must be adopted. Finally, the control strategies must be robust – for example, high-bandwidth communications requirement may pose problems, especially because, in case of WMD attack, communications networks may become congested or even inoprable.

In this work, we made the assumption that thermal storage devices were installed in either 50% or 100% of commercial buildings. This is a cost-effective strategy for

controlling the load profile on the network, and represents the largest individual component of the peak load. However, similar considerations would apply to electrical storage, which is in fact subject to less stringent requirements, since power flow is bidirectional. We considered two strategies for load control – real-time price and stochastic.

With real-time price control, the cost of power is a function of the residual capacity of the system. This is in line with industry practices, and is also compatible with WMD response, since a WMD attack would automatically result in reduced capacity. The customers use automated response to activate their storage devices. Thermal load is either met by depleting storage or by purchasing power from the network, depending on an internal power price threshold. The threshold for meeting thermal load, in turn, is set based on the state of charge of the storage – a high threshold when state of charge is low, and vice versa. The threshold for charging is set similarly.

Stochastic control (SC) could be used in regions where RTP is not allowed by regulation. In this case, the utility or some control agency would send a signal to all customers, between 0 and unity, representing the probability of activating a distributed resource. In turn, each resource generates a random number, which is compared with the utility signal. Based on the result of the comparison, the device is either activated or not. With stochastic control, loads can choose to op-in, and be financially compensated as a result.

Our results have shown that both RTP and SC are effective means of controlling the total load on the grid, and can respond effectively to both renewable energy intermittency and load shedding requests. Moreover, the bandwidth for communication is very low – only requiring a common signal to be broadcast at regular intervals, typically on the order of minutes. We also note that these same mechanisms could be used for enhanced readiness to WMD threats. For example, it is possible to increase the storage SOC in cases of enhanced threat, simply by modifying the RTP or the stochastic signal. In other words, the operating mode of the network could be modified by using "normal" control procedures, in response to the risk of cascading failure identified using the methodology described in other component of this report.

We also performed simulations to reveal the effects of the control/communication system parameters on the cascading failures in power grids. Our simulations have shown that vulnerabilities in the control/communication systems can increase the probability of large cascading failures initiated by small disturbances over the power grid. In addition, we observed that the topological location and characteristics of the failures affect the cascading behaviors in the power grid. Since inhibition and clustering can be important attributes of WMD attacks, which exhibit great level of spatial correlation, we looked at the effects of spatial inhibition and clustering among the uncontrollable load buses. These effects can be important due to the nature of certain disaster events that may affect the

power grid and their control/communication systems. We observed that cascading failures are more likely in scenarios where there is inhibition (negative spatial correlation) in the loads for which we lose control over than that for scenarios where there is a clustering effect (positive spatial correlation) in these loads.

5. Personnel Supported

Faculties and researchers:

- Dr. Majeed M. Hayat, PI, UNM
- Dr. Andrea Mammoli, Co-PI, UNM
- Dr. Yasamin Mostofi, Co-PI, UNM
- Dr. Patrick Bridges, Co-PI, UNM

Students:

- Mahshid Rahnamay-Naeini, Ph.D. student in Electrical and Computer Engineering, UNM
- Zhuoyao Wang, Dosanjh
- Matthew Dosanjh, Ph.D. student in Computer Science
- Yaser Yasei, Ph.D. student in Electrical and Computer Engineering
- Shahin Abdollahy, Ph.D. student in Electrical and Computer Engineering

6. Publications

1. M. Rahnamay-Naeini, Z. Wang , A. Mammoli , and M. M. Hayat, "A Probabilistic Model for the Dynamics of Cascading Failures and Blackouts in Power Grids," *IEEE PES General Meeting*, San Diego, CA, 2012, accepted.

2. A. Mammoli, B. Jones, H. Barsun, D. Dreisigmeyer, G. Goddard, O. Lavrova, " Distributed Control Strategies for High-Penetration Commercial-Building-Scale Thermal Storage
Author: Session: ICGG Smart Grid Applications," *Proceedings of IEEE-PES Transmission & Distribution Meeting*, Orlando, FL, May 2012.

3. M. Rahnamay-Naeini, Z. Wang , A. Mammoli , and M. M. Hayat, "Impacts of Inefficient Load Shedding on Power Systems Operating Under Vulnerable Conditions," *IEEE PES General Meeting*, San Diego, CA, 2012, accepted.

7. Interactions/Transitions

7.1 Meetings, Conferences, etc.

- Drs. Hayat, Mammoli, Mostofi and Bridges presented the findings of this research project to at the DTRA University Partnership Program—Site Visit, Albuquerque, NM July 7th, 2011.
- Drs. Hayat and Mammoli have presented the findings of this research project to PM Dr. Kehlet and his colleagues at DTRA, Virginia, August 2011.
- Dr. Mammoli has presented a paper to the IEEE-PES Transmission & Distribution Meeting, Orlando, FL, May 2012.

8. Honors/Awards

- In 2011, Dr. Yadamin Mostofi received the National Science Foundation's Presidential Early Career Award for Scientists and Engineers (PECASE).
- In May 2012, graduate student Mahshid Rahnamay-Naeini received the IEEE Outstanding Graduate Engineering Student Award (IEEE Region 6, Albuquerque Section) for her work in this project on cascading failures in power grids.
- In December 2012, Dr. Hayat was elevated to the grade of SPIE Fellow.

9. References

1. M. Rahnamay-Naeini, Z. Wang , A. Mammoli , and M. M. Hayat, "A Probabilistic Model for the Dynamics of Cascading Failures and Blackouts in Power Grids," *IEEE PES General Meeting*, San Diego, CA, 2012, accepted.

2. A. Mammoli, B. Jones, H. Barsun, D. Dreisigmeyer, G. Goddard, O. Lavrova, " Distributed Control Strategies for High-Penetration Commercial-Building-Scale Thermal Storage
Author: Session: ICGG Smart Grid Applications," *Proceedings of IEEE-PES Transmission & Distribution Meeting*, Orlando, FL, May 2012.

3. M. Rahnamay-Naeini, Z. Wang , A. Mammoli , and M. M. Hayat, "Impacts of Inefficient Load Shedding on Power Systems Operating Under Vulnerable Conditions," *IEEE PES General Meeting*, San Diego, CA, 2012, accepted.

4. R. Zimmerman, C. Murillo-Sanchez, and D. Gan, *MATLAB Power System Simulation Package*, Version 4.0b4 ed., May 2010.

10. Appendix

Reprints of three publications resulting from this project. (See next pages.)

DEPARTMENT OF DEFENSE

DEFENSE THREAT REDUCTION
AGENCY
8725 JOHN J. KINGMAN ROAD
STOP 6201
FORT BELVOIR ,VA 22060
ATTN: J. REED

DEFENSE THREAT REDUCTION
AGENCY
8725 JOHN J. KINGMAN ROAD
STOP 6201
FORT BELVOIR ,VA 22060
ATTN: R. KEHLET

DEFENSE TECHNICAL
INFORMATION CENTER
8725 JOHN J. KINGMAN ROAD,
SUITE 0944
FT. BELVOIR, VA 22060-6201
ATTN: DTIC/OCA

DEPARTMENT OF DEFENSE CONTRACTORS

EXELIS, INC.
1680 TEXAS STREET, SE
KIRTLAND AFB, NM 87117-5669
ATTN: DTRIAC

OFFICE OF THE VICE PRESIDENT
FOR RESEARCH
UNIVERSITY STRATEGIC
PARTNERSHIP MSCO2 1660
1 UNIVERSITY OF NEW MEXICO
ALBUQUERQUE, NM 87131